

# Gaussian process modelling of austenite formation in steel

C. A. L. Bailer-Jones, H. K. D. H. Bhadeshia, and D. J. C. MacKay

The present paper introduces the Gaussian process model for the empirical modelling of the formation of austenite during the continuous heating of steels. A previous paper has examined the application of neural networks to this problem, but the Gaussian process model is a more general probabilistic model which avoids some of the arbitrariness of neural networks, and is somewhat more amenable to interpretation. It is demonstrated that the model leads to an improvement in the significance of the trends of the  $Ac_1$  and  $Ac_3$  temperatures as a function of the chemical composition and heating rate. In some cases, these predicted trends are more plausible than those obtained with the neural network analysis. Additionally, it is shown that many of the trace alloying elements present in steels are irrelevant in determining the austenite formation temperatures.

MST/4132

At the time the work was carried out Dr Bailer-Jones was in the Cavendish Laboratory, Department of Physics and in the Department of Materials Science and Metallurgy, University of Cambridge, UK. Dr Bhadeshia is in the Department of Materials Science and Metallurgy and Dr MacKay is in the Cavendish Laboratory, Department of Physics at the University of Cambridge, UK. Dr Bailer-Jones is now at the Max Planck Institut für Astronomie, Koenigstuhl 17, D-69117, Heidelberg, Germany. Manuscript received 29 May 1998.

© 1999 IoM Communications Ltd.

## Introduction

The formation of austenite is an important component in the heat treatment of steels. The temperature at which austenite begins to form during the continuous heating of steel is termed the  $Ac_1$  temperature, and that at which the steel becomes fully austenitic is the  $Ac_3$  temperature. The corresponding equilibrium temperatures (i.e. those for an infinitesimally small heating rate) are  $Ae_1$  and  $Ae_3$ , respectively, with  $Ac_1 \geq Ae_1$  and  $Ac_3 \geq Ae_3$ . In previous work (hereafter referred to as GBMS),<sup>1</sup> a neural network was used to model the variation in these transformation start and finish temperatures as a function of the steel chemical composition and the heating rate (the ‘inputs’). The analysis was conducted on a large data set compiled from the published literature, taking into account a total of 21 different alloying elements.

Generally, the trained neural network was demonstrated to be largely consistent with phase transformation theory, and its predicted trends (i.e. the variation of  $Ac_1$  and  $Ac_3$  with the inputs) agreed with established metallurgical understanding. However, in some cases the trends were found to be uncertain (large error bars) and hence difficult to interpret, and in a few cases the trends differed considerably from what was expected. Subsequent use of the model has also revealed that the analysis may have been over ambitious in the number of composition terms included as input variables: many of the trace elements showed little or no significant variation within the data set used to develop the network. Thus, the model was unable to learn the dependence of  $Ac_1$  and  $Ac_3$  on these trace elements, and as a consequence the model tended, not surprisingly, to give uncertain predictions when the trace element concentrations were varied.

The present work has two aims. The first is to repeat the analysis using a reduced set of variables by eliminating those variables which (a) show very little variation, (b) are believed not to influence significantly the austenite formation process at the concentrations involved, or (c) are likely to have been inaccurately determined.

The second aim is to introduce a more general method of data modelling, the Gaussian process model.<sup>2,3</sup> The neural network method in the original work involved the creation of a large set of models, each with a different level of complexity. Those models that were too simple, and

hence unable to capture the trends in the data, were rejected, as were over complex models which did not generalise well. Thus, considerable effort was expended in determining the required complexity of the function (network) describing the relationship between the input and output variables. The Gaussian process model, on the other hand, avoids the explicit parameterisation of the input–output function. One of the advantages of this is that it does not require an often *ad hoc* decision regarding the complexity of the model (i.e. the number of hidden nodes and layers in the network). It has been shown that the Gaussian process is a generalisation of many standard interpolation methods, including neural networks and splines.<sup>4</sup> In metallurgy, Gaussian processes have been applied to the problem of modelling recrystallisation in aluminium alloys.<sup>5,6</sup>

In the present work, a Gaussian process model is trained on the reduced data set, and the results compared with those from the neural network in GBMS. To ascertain whether the differences arise from the use of a new type of model or the reduced data set, another Gaussian process model is trained on the full data set (i.e. all 22 input variables) used in GBMS.

## Data

The original data set consisted of 22 input variables and two output variables, namely, the  $Ac_1$  and  $Ac_3$  temperatures which describe the onset and completion, respectively, of austenite formation during continuous heating from ambient temperature. A total of 788 cases (input–output pairs) were used in the analysis.

In addition to the heating rate, the input variables consisted of the elements C, Si, Mn, Cu, Ni, Cr, Mo, Nb, V, W, and Co, together with the trace elements S, P, Ti, Al, B, As, Sn, Zr, N, and O. However, a close examination of the dataset indicated that the variation in concentration for the trace elements was rather small (zero in the cases of As, Sn, Zr, and O) and possibly insignificant compared with the estimated precision of the chemical analysis. Furthermore, in the majority of cases, the trace elements are in such small concentrations that they are not expected to have a great influence on the transformation behaviour. They were therefore eliminated from the list of inputs. The reduced data set is presented in Table 1.

## Data modelling

The problem addressed is one of obtaining a model of the dependence of an ‘output’ variable, such as the  $Ac_1$  temperature, on several input variables, such as the mass fractions of the different alloying elements. A general approach to this type of problem is to formulate a physically motivated, parameterised model which describes the relationship between the inputs and the output. The parameters of the model can then be inferred using a set of measured inputs and outputs (the training data), i.e. these data are interpolated. This can be done with standard regression methods such as least squares minimisation. Once the parameters have been determined, predictions of the output can be made for any values of the inputs. However, such an approach is limited to those simple problems for which a physical model can be devised that still models the data with sufficient accuracy. To obtain accurate predictions in more complex situations, it is often necessary to take an empirical approach, in which the input–output relationship is determined from the data without reference to a simplified physical model.

One such approach is neural network modelling. Neural networks are a flexible approach to data modelling as they can provide an arbitrarily complex, non-linear mapping between one or more inputs and an output. This mapping is parameterised by a set of ‘weights’, the optimum values of which are determined by training the network.

## Gaussian process model

In modelling complex problems empirically, it is not known what the parameterised form of the input–output relationship should be. The Gaussian process model is a way of avoiding having to parameterise this relationship explicitly by instead parameterising a probability model over the data.<sup>2,3</sup>

Let the training data set consist of  $N$  input vectors  $\{x_1, x_2, \dots, x_N\}$  and the corresponding set of known outputs or ‘targets’ be  $\{t_1, t_2, \dots, t_N\}$ . A prediction  $t_{N+1}$  can then be made at any new input value  $x_{N+1}$ , based on these training data. For brevity, let  $X_N$  represent the set of input vectors and  $t_N$  be the vector of corresponding outputs.

The approach of the Gaussian process model is as follows. Let  $P(t_N|x_N)$  be the joint probability distribution over the  $N$  output values in the training data set. This is a probability distribution in an  $N$ -dimensional space. Similarly, the joint probability distribution of both the  $N$  training data points and the single new point is

**Table 1** Reduced data set: the 12 input variables consist of 11 element concentrations (wt-%) and heating rate; the two output variables are  $Ac_1$  and  $Ac_3$  temperatures

Variable	Range	Mean	Standard deviation
C	0–0.96	0.30	0.17
Si	0–2.13	0.39	0.41
Mn	0–3.06	0.82	0.38
Cu	0–2.01	0.05	0.13
Ni	0–9.12	1.01	1.48
Cr	0–17.98	1.23	2.38
Mo	0–4.80	0.32	0.37
Nb	0–0.17	0.003	0.013
V	0–2.45	0.05	0.13
W	0–8.59	0.06	0.48
Co	0–4.07	0.06	0.42
Heating rate, K s <sup>–1</sup>	0.03–50	1.0	11.6
$Ac_1$ , °C	530–921	724	52
$Ac_3$ , °C	651–1060	819	55

$P(t_{N+1}, t_N|x_{N+1}, X_N)$ . In making predictions based on the training data, it is necessary to find  $P(t_{N+1}|x_{N+1}, D)$ , that is, the probability distribution over the predicted point given that the corresponding input  $x_{N+1}$  and all of the training data  $D = \{t_N, X_N\}$  are known. The relationship between these quantities comes from the simple rule of probability,  $P(A, B) = P(A|B)P(B)$ , which in this case translates to

$$P(t_{N+1}|x_{N+1}, D) = \frac{P(t_{N+1}, t_N|x_{N+1}, X_N)}{P(t_N|X_N)} \quad \dots \quad (1)$$

To evaluate this, it is necessary to choose the form of these probability distributions. The Gaussian process model specifies that the joint prior probability distribution of any  $N$  output values is a multivariate Gaussian

$$P(t_N|X_N, \Theta) \propto \exp \left[ -\frac{1}{2} (t_N - \mu)' C_N^{-1} (t_N - \mu) \right] \quad (2)$$

where  $\mu$  is the mean and  $C_N$  is a covariance matrix which is a function of  $X_N$  and  $\Theta$ , the latter being a set of parameters that are discussed below. A similar equation holds for  $t_{N+1}$ , where  $t_{N+1} = (t_N, t_{N+1})$ . Thus, it can be seen that the numerator and denominator in equation (1) are multivariate Gaussians of dimension  $N+1$  and  $N$ , respectively, in which case it can be shown that  $P(t_{N+1}|x_{N+1}, D)$  is a univariate Gaussian

$$P(t_{N+1}|x_{N+1}, D) = \frac{1}{(2\pi)^{1/2} \sigma_i} \exp \left[ -\frac{(t_{N+1} - \hat{t})^2}{2\sigma_i^2} \right] \quad (3)$$

with mean  $\hat{t}$  and standard deviation  $\sigma_i$ . This is the desired probability distribution over the output value for the given input  $x_{N+1}$ . (Note that this does not indicate that the input–output function itself is a Gaussian.) As this is an entire probability distribution, not only can a prediction be made, but confidence intervals can also be assigned to this prediction. Typically, a prediction would be reported as  $\hat{t} \pm \sigma_i$ , where  $\sigma_i$  is the  $1\sigma$  error determined by the model.

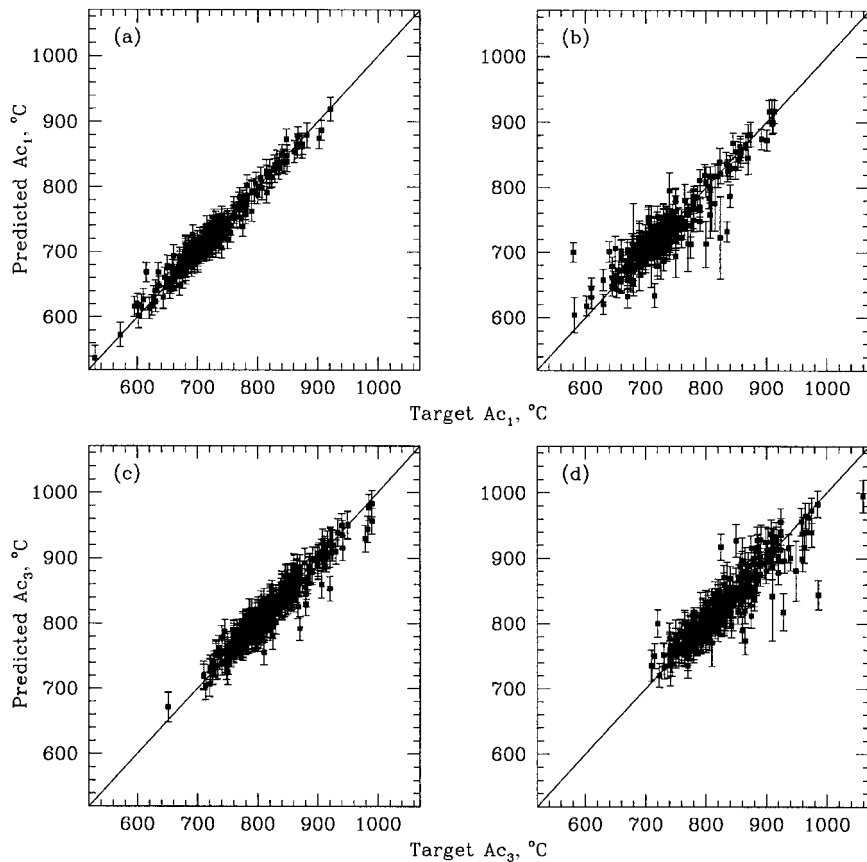
The values of  $\hat{t}$  and  $\sigma_i$  depend on the covariance matrix  $C_N$  of the Gaussian process model in equation (2) (see Appendix). The elements of this matrix  $C_{ij}$  are given by the covariance function  $C$ . The form of the covariance function is central to the Gaussian process model, and embodies the assumptions about the nature of the underlying input–output function to be modelled. It is through the covariance function that the predictions depend upon the inputs in the training data.

The covariance function used is

$$C = \theta_1 \exp \left[ -\frac{1}{2} \sum_{l=1}^{L=1} \frac{(x_i^{(l)} - x_j^{(l)})^2}{r_l^2} \right] + \theta_2 + \sigma_n^2 \delta_{ij} \quad (4)$$

This gives the covariance between any two output values  $t_i$  and  $t_j$ , with corresponding  $L$  dimensional input vectors  $x_i$  and  $x_j$ , respectively. The first term in  $C$  specifies the belief that the underlying function being modelled is smoothly varying:  $r_l$  is the characteristic length scale over which the function varies in the  $l$ th input dimension. Examining the form of this term, it can be seen that when two inputs are ‘close’ (with respect to their length scales) the exponent is small, so this term makes a large contribution to the covariance. In other words, if two input vectors are close, their corresponding outputs are highly correlated, making it probable that they have similar values. This form of  $C$  places relatively few constraints on the function, and permits the modelling of non-linear functions.

The second term in equation (4) simply allows functions to have a constant offset, i.e. have a mean different from zero. (This could also be done by setting the mean in equation (2) to  $\mu = (1, 1, \dots, 1)c$ , where  $c$  is a hyperparameter that must be inferred. Instead, it has been chosen to set  $\mu = 0$  and have all of the hyperparameters in the covariance function.) The final term is the noise model:  $\delta_{ij}$  is the delta function, so this term gives a contribution to the covariance



a  $Ac_1$  model predictions of training data,  $E = 11.3^\circ\text{C}$ ; b  $Ac_1$  model predictions of test data,  $E = 20.9^\circ\text{C}$ ; c  $Ac_3$  model predictions of training data,  $E = 15.4^\circ\text{C}$ ; d  $Ac_3$  model predictions of test data,  $E = 22.7^\circ\text{C}$

**1 Predicted versus target outputs for  $Ac_1$  and  $Ac_3$  Gaussian process models trained on reduced data set:  $E$  is root mean square (rms) value of predictions in each case, i.e. scatter of points about the overplotted predicted = target line; the error bars  $\sigma_i$  are the modelling uncertainties predicted by the Gaussian process model (equation (3))**

only when  $i = j$ . This case is a constant (input independent) noise model; the variance of the noise is  $\sigma_n^2$ . Note that this noise model is for the outputs only: the inputs are assumed to be noise free.

The set of parameters  $r_l$  ( $l = 1 \dots L$ ),  $\theta_1$ ,  $\theta_2$ , and  $\sigma_n$  in equation (4) are termed hyperparameters because they explicitly parameterise a probability distribution over the input-output function rather than the function itself. They will be denoted  $\Theta$  for brevity, as in equation (2). Along with  $x_{N+1}$  and the training data, the hyperparameters completely specify the elements of the covariance matrix and hence the values of  $\hat{t}$  and  $\sigma_i$  (see Appendix).

If enough is known about the problem, these hyperparameters can be set by hand. More commonly, however, their optimum values must be inferred from the training data. This is done by maximizing  $P(\Theta|D)$ , the probability of the hyperparameters given the training data, with respect to  $\Theta$ . This is related to  $P(t_N|X_N, \Theta)$  in equation (2) via Bayes's theorem

$$P(\Theta|D) = \frac{P(t_N|X_N, \Theta)P(\Theta)}{P(t_N|X_N)} \quad \dots \quad \dots \quad \dots \quad \dots \quad \dots \quad (5)$$

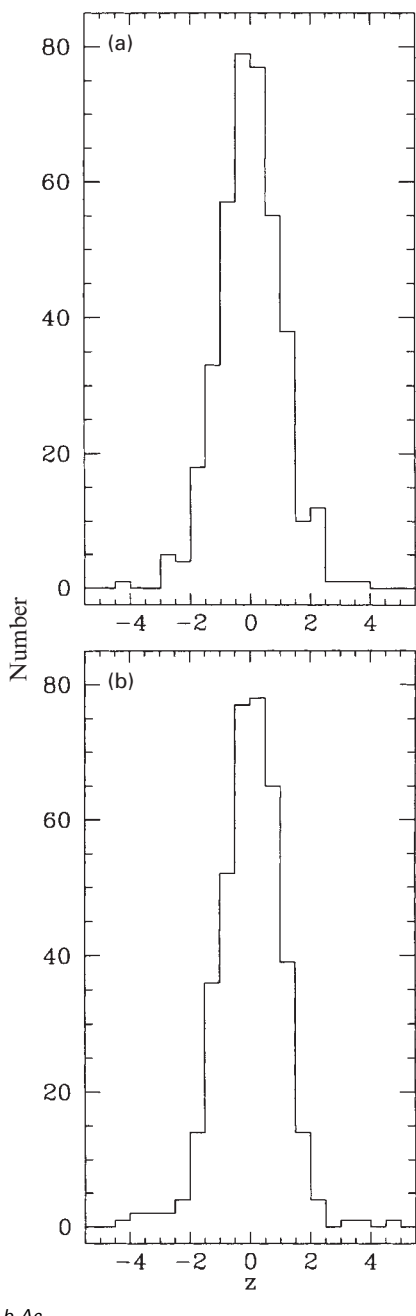
The optimisation must usually be done numerically. The second term in the numerator of equation (5) is the prior probability distribution over the hyperparameters. The hyperparameter priors are an important method for introducing any prior knowledge of the values of the length scales, or the magnitude of the noise variance. This approach of maximising the evidence for the hyperparameters is a Bayesian one which automatically embodies complexity control, even if the prior on the hyperparameters is uniform (uninformative).<sup>7</sup>

## Results

### MODEL PERFORMANCE

In developing a Gaussian process model, the data set was randomly divided into two halves, each consisting of 394 input-output pairs. The first half (training data) was used to train the model, and the second half (test data) was then used to test the ability of the model to generalise its predictions. To aid interpretation of the model, each input and output variable was linearly scaled into the range  $-0.5$  to  $+0.5$ , using the range values given in Table 1.

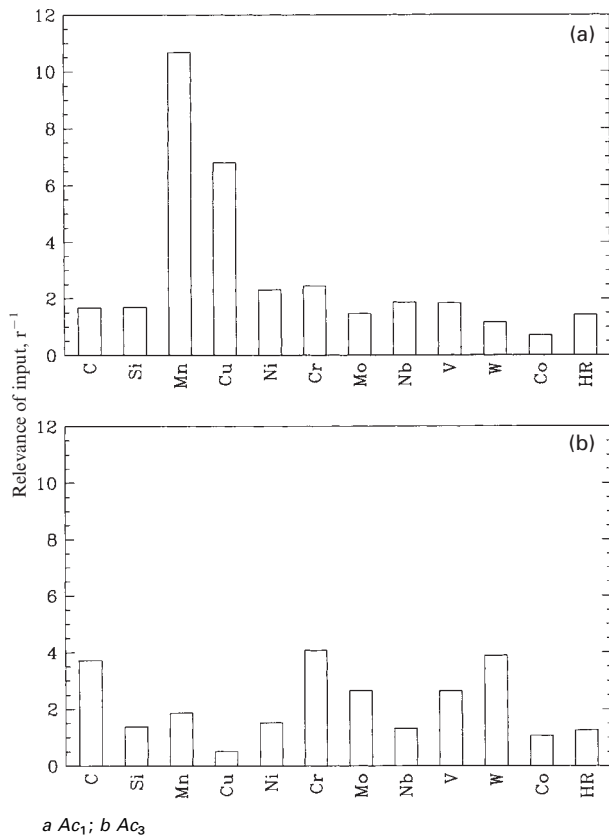
Two separate Gaussian process models were developed in this fashion, one to model each of  $Ac_1$  and  $Ac_3$  as a function of the reduced input data set (Table 1). The performance of these models on the training and the test data is shown in Fig. 1, by plotting the predicted value  $\hat{t}$  against the target value  $T$ . Figure 1 clearly demonstrates that both models have generalised well, and therefore have captured the underlying relationships in the training data. These plots also show the modelling uncertainties  $\sigma_i$  determined by the model (equation (3)). The size of these uncertainties is commensurate with the scatter of the predictions about the target values, giving confidence that the model is making good predictions of its own error. This can be better seen in Fig. 2, which shows histograms of the  $z$  values. The  $z$  value is the number of standard deviations from which the predicted value differs from the target value, i.e.  $z = (\hat{t} - T)/\sigma_i$ . Figure 2 indicates that the model is predicting reasonable uncertainties, with 94% (68%) of both  $Ac_1$  and  $Ac_3$  predicted temperatures lying within  $2\sigma_i$  ( $1\sigma_i$ ) of the target value.



**2 Histograms of  $z = (t - T)/\sigma_t$  for  $Ac_1$  and  $Ac_3$**

Figure 3 shows the inverses of the length scale hyperparameters for the two Gaussian process models. As can be seen from equation (4), the inverse square of the length scale  $r_l$  gives the scale of the  $l$ th input over which the output varies by a significant amount. Thus,  $r_l^{-1}$  is a measure of the ‘relevance’ of the  $l$ th input in determining the output: if  $r_l$  is small, the output varies considerably as  $x_l$  does, so its relevance is large. Note that the relevance is not quite the same as ‘sensitivity’ of the output  $t$  to an input  $x_l$ . (This latter quantity would be  $\partial t / \partial x_l$ , which depends on the value of  $x_l$ .) Rather, the relevance is an overall measure of the significance of that input variable in determining the output. The relevance parameters can be compared directly with the  $\sigma_w$  values in GBMS, and show similar overall results.

According to Fig. 3, the models predict that carbon explains less of the variation in  $Ac_1$  than in  $Ac_3$ . This can be understood physically because the carbon is, in the starting microstructure, present as carbides, with very little of



**3 Model inferred relevance of 12 inputs for the  $Ac_1$  and  $Ac_3$  Gaussian process models: HR is heating rate; the relevances are inverses of length scales  $r_l$**

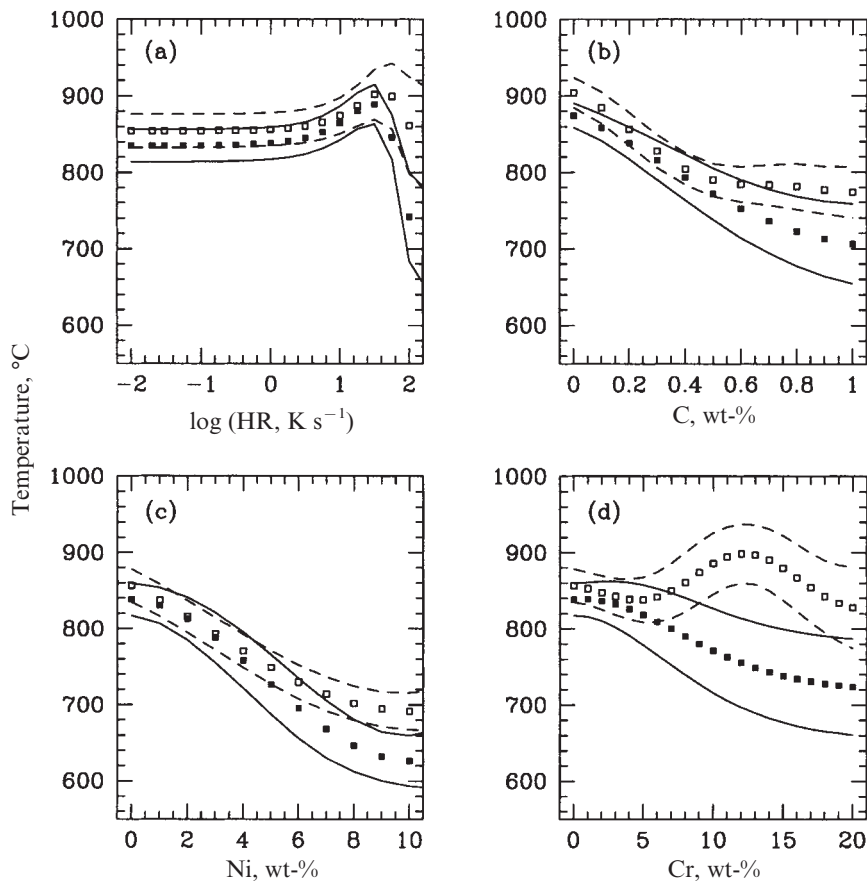
it in solution. The average carbon concentration is therefore of secondary importance for the start of austenite formation.

It is important to note that the length scales reported in Fig. 3 are in units of the scaled input variable. As the inputs were scaled to lie in the range  $-0.5$  to  $+0.5$ , the size of the length scale depends on the range of the inputs. Thus, the reported length scale of 1.68 for carbon in the  $Ac_1$  problem corresponds to a length scale in units of concentration of 1.61 wt-%, whereas the almost identical reported length scale of 1.69 for silicon corresponds to a concentration length scale of 3.60 wt-%, on account of the larger range of concentrations of silicon in the data set (Table 1). None the less, it is useful to report length scales in terms of the scaled variable, as this takes into account the differences in the typical concentration ranges of the different alloying elements.

The standard deviation of the noise in the data  $\sigma_n$  is one of the hyperparameters learned by the model during training (see equation (4)). This was found to be  $\sigma_n = 14.0^\circ\text{C}$  and  $\sigma_n = 17.5^\circ\text{C}$  for the  $Ac_1$  and  $Ac_3$  models, respectively. The noise, along with some additional ‘fitting uncertainty’, comprises the modelling uncertainty  $\sigma_i$  at a given point (the error bars in Fig. 1). The average value of  $\sigma_i$  for the test data is  $17.3^\circ\text{C}$  and  $19.7^\circ\text{C}$  for  $Ac_1$  and  $Ac_3$ , respectively. Assuming that the fitting uncertainty and noise add in quadrature, it can be seen that the noise typically contributes  $\sim 85\%$  of the total modelling uncertainty. In other words, the intrinsic noise in the measurements of  $Ac_1$  and  $Ac_3$  is probably the dominant source of error.

## MODEL PREDICTIONS

Figures 4–6 show the models’ predictions of the effects of varying the concentration of the different alloying elements on the  $Ac_1$  and  $Ac_3$  temperatures. Other than the predicted



■  $Ac_1$  predictions; —  $Ac_1 \pm 1\sigma$  modelling uncertainties; □  $Ac_3$  predictions; ---  $Ac_3 \pm 1\sigma$  modelling uncertainties  
a HR, Fe-0.2C; b C,Fe-C, 1 K s<sup>-1</sup>; c Ni,Fe-0.2C, 1 K s<sup>-1</sup>; d Cr,Fe-0.2C, 1 K s<sup>-1</sup>

#### 4 Gaussian process model predictions for heating rate (HR), C, Ni, and Cr for given alloys and heating rate

trends shown in Fig. 4 for carbon and the heating rate, all predictions are for a heating rate of 1 K s<sup>-1</sup> and for Fe-0.2C (wt-%) steels, i.e. the fraction of all alloying elements other than that being varied is zero. The predicted effect of the carbon concentration (Fig. 4b) is for a plain carbon steel (i.e. binary Fe-C alloys), again at a heating rate of 1 K s<sup>-1</sup>. The heating rate prediction (Fig. 4a) is for a binary Fe-0.2C steel.

The peak in the transformation temperature (Fig. 4a) was not initially expected, although it can be explained if retained austenite is present in the microstructure. This prediction is consistent with that given by the neural network in GBMS, and the reader is referred to that paper for a discussion.<sup>1</sup> The predictions for carbon (Fig. 4b) are in broad agreement with those obtained in GBMS.

Nickel is an austenite stabiliser and, judging from the phase diagram, both the  $Ac_1$  and the  $Ac_3$  temperatures should decrease with increasing nickel concentration. These trends are predicted by the Gaussian process models as illustrated in Fig. 4c. This result is a large improvement over the results of the previous neural network analysis, which not only gave an incorrect trend for the  $Ac_1$  temperature as a function of the nickel concentration, but also indicated very large uncertainties in the calculations.

The predictions for chromium (Fig. 4d) are more interesting and, again, differ significantly from GBMS. The  $Ac_3$  temperature goes through a minimum at ~5 wt-%Cr, which is consistent with a minimum found in the equilibrium  $Ae_3$  temperature at ~7 wt-%. On the other hand, the trend of  $Ac_1$  as a function of chromium is opposite to that expected for  $Ae_1$ ; the reason for this is not understood.

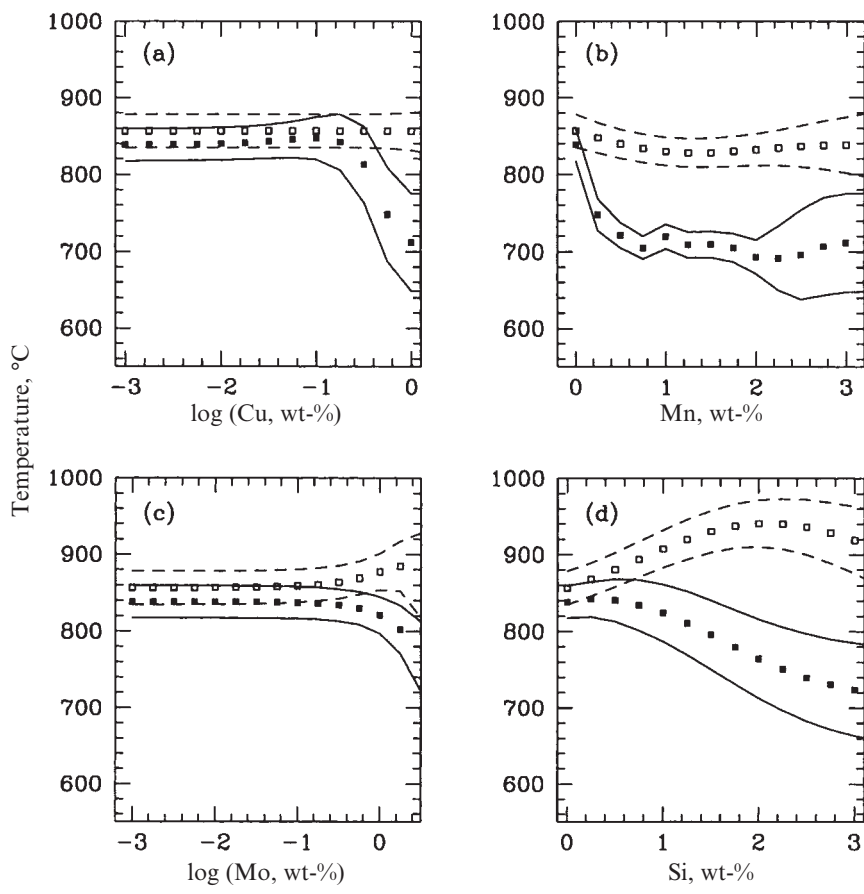
It would be useful to know whether these discrepancies between the Gaussian process model and the neural network model are on account of having used a different

model or the reduced data set. To determine this, Gaussian process models based on the full data set used in GBMS were developed and used to make predictions for the same alloys. For brevity, the Gaussian process model trained on the reduced data set will be referred to as the 12D model (for 12 input dimensions) and that trained on the full data set as the 22D model. Both models give essentially identical trends with heating rate, carbon, and nickel for both  $Ac_1$  and  $Ac_3$ , indicating that the improved predictions shown in Fig. 4 are on account of having used the Gaussian process model rather than the removal of the trace elements.

Figure 5a shows that copper, over the concentration range considered, has little influence on the  $Ac_3$  temperature but depresses the  $Ac_1$  temperature as the concentration approaches the upper limit of ~1 wt-%. The latter effect is expected from the phase diagram, as copper increases the stability of austenite.

The Gaussian process predictions for manganese are similar to those obtained by the neural network, but the larger uncertainties predicted by the Gaussian process seem more reasonable. This is particularly the case when considering that the model should never predict uncertainties smaller than the inferred noise level. Figure 5b shows some 'high frequency' detail in the variation of the  $Ac_1$  predictions for manganese, which is not expected and was not present in the neural network predictions. This is reflected by the small length scale (0.09) for the Gaussian process model. In comparison, the 22D Gaussian process model predicts less variation, and has a correspondingly larger length scale (0.22). The discrepancy may be on account of the 12D model slightly overfitting the data in this region of the input space.

The  $Ac_1$  and  $Ac_3$  temperatures show a similar insensitivity to low concentrations of molybdenum as in the previous



$\blacksquare$   $Ac_1$  predictions; —  $Ac_1 \pm 1\sigma$  modelling uncertainties;  $\square$   $Ac_3$  predictions; ---  $Ac_3 \pm 1\sigma$  modelling uncertainties  
a Cu; b Mn; c Mo; d Si

##### 5 Gaussian process model predictions for Cu, Mn, Mo, and Si: alloys are Fe-0.2C steels, heating rate is $1\text{ K s}^{-1}$

work (Fig. 5c). As noted in GBMS, the opposite trends of  $Ac_1$  and  $Ac_3$  at higher concentrations are consistent with phase diagram calculations. The 22D Gaussian process model gives essentially identical predictions.

It is worth mentioning at this point that the Gaussian process model, like the neural network, is an interpolation model. Thus, when extrapolating beyond the ranges of the input values in the training data set, the predictions are less well determined by the data, so poorer the predictions would be expected. Correspondingly, the model would be expected to predict larger uncertainties, and this can be seen in Figs. 4 and 5. Moving away from the range of the training data, the predictions become more and more model dependent, in this case dependent on the form of the covariance function. Inspection of equation (4) shows that, well away from the data (large  $x_i$ ), the dominant covariance term is  $\theta_2$ , which is constant, so the extrapolations will tend asymptotically towards a constant value. The predictions in Figs. 4–6 are mostly for values within the range of inputs. However, it should be pointed out that the distribution of the inputs is sometimes skewed towards low values, e.g. for molybdenum (Table 1). Thus, although it seems possible that model dependent extrapolation could explain the ‘turn down’ in  $Ac_1$  for high molybdenum concentrations in Fig. 5c, this is unlikely, as a similar turn down is seen in GBMS from the neural network, which has a different model prior. The present authors are similarly confident that much of the behaviour in the other plots is ‘real’.

An initial reaction may be that extrapolations should follow the last trend in the data, rather than tending towards a constant value. However, it can not necessarily be justified that such trends influence predictions at very distant parts of the parameter space. The choice of the

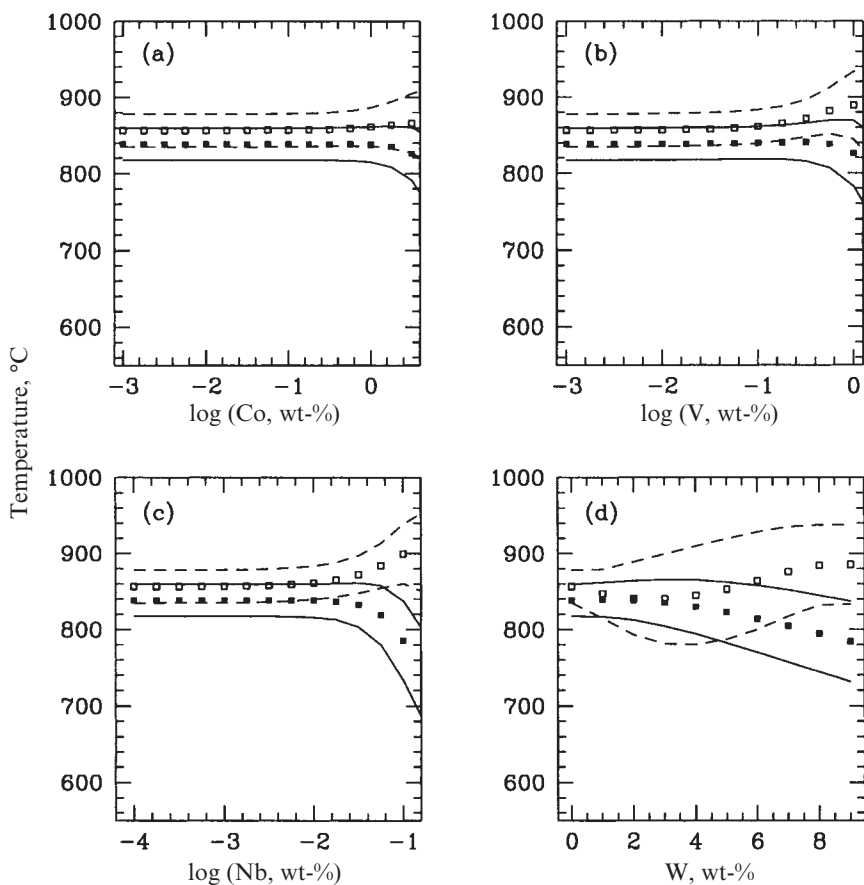
model prior is thus somewhat philosophical, and will not be discussed here. It is sufficient to note that the extrapolation from any model will be model dependent. A different Gaussian process covariance function could be introduced to provide different extrapolation behaviours.<sup>8</sup>

The Gaussian process model gives a predicted trend for the  $Ac_1$  temperature with silicon (Fig. 5d) which differs from the neural network predictions. However, given the very large error bars in the latter case, the neural network essentially failed to learn any significant trend. The 22D Gaussian process models give similar predictions and error bars to those of the 12D Gaussian process models, showing that the reduced uncertainty is a result of using the Gaussian process model.

The  $\gamma + \alpha$  phase field in Fe-Co alloys is extremely narrow and the phase boundaries are virtually horizontal on the plot of temperature versus concentration. This is accurately reflected in the predictions for cobalt (Fig. 6a). Vanadium is a very strong carbide forming element, with limited solubility even in austenite. Hence, it is not surprising that both the  $Ac_1$  and the  $Ac_3$  temperatures are insensitive to the vanadium concentration (Fig. 6b). This is similar to the predictions of GBMS, but the Gaussian process model does not predict the sharp increase in both  $Ac_1$  and  $Ac_3$  between concentrations of 0.1 and 1.0 wt-%. The 22D Gaussian process models show very similar behaviour to that of the 12D Gaussian process models.

##### Model comparison

The performance of the models discussed above (12D Gaussian process model; 22D Gaussian process model;



■  $Ac_1$  predictions; —  $Ac_1 \pm 1\sigma$  modelling uncertainties; □  $Ac_3$  predictions; ---  $Ac_3 \pm 1\sigma$  modelling uncertainties  
a Co; b V; c Nb; d W

## 6 Gaussian process model predictions for Co, V, Nb, and W: alloys are Fe-0.2C steels, heating rate is $1\text{ K s}^{-1}$

neural network model from GBMS) can be assessed by comparing root mean square (rms) errors on the test data. These are given in Table 2. The models give very similar rms errors for the  $Ac_1$  problem. This indicates that removing the 10 trace variables does not decrease the quality of the predictions. It also shows that there is little difference in the average performance of the models, although the above analysis has shown that the Gaussian process models give better predictions (as well as more plausible error bars) for some Fe-0.2C steels.

The smaller  $Ac_3$  error for the 12D Gaussian process model, compared to the 22D Gaussian process model, is presumably on account of having removed the trace variables. This would seem to confirm the suspicion that retaining the trace variables leads to inferior performance, probably owing to the inaccuracy of their measurement. It is interesting, however, that this has not affected the  $Ac_1$  Gaussian process model. It is possible that the trace variables are more significant in determining  $Ac_1$  than  $Ac_3$ .

**Table 2 Comparison of root mean square (rms) errors  $E$  and log predicted errors  $\ln L$  for test data obtained by three different models: neural network model is from GBMS;<sup>1</sup> in all cases one of inputs is heating rate, other inputs are alloying elements**

Model	$E(Ac_1)$ , °C	$E(Ac_3)$ , °C	$\ln L(Ac_1)$	$\ln L(Ac_3)$
Neural network (22 input dimensions)	20.2	21.8	...	...
Gaussian process (22 input dimensions)	21.0	25.3	971	954
Gaussian process (12 input dimensions)	20.9	22.7	967	964

but the reduction for  $Ac_3$  is small ( $2.6\text{ }^\circ\text{C}$ ), so this conclusion may not be particularly significant.

The rms error does not tell the entire story, as it ignores the predicted error  $\sigma_i$ . Thus, even if a prediction that differs greatly from its target value has a correspondingly large predicted uncertainty, it will nevertheless make a large contribution to the rms error. This limits the value of the rms error as a measure of model performance. A measure that does take into account the predicted uncertainties is  $P(t_{N+1}|x_{N+1}, D)$  in equation (3), the probability of a prediction given the training data. The product of these probabilities over the  $K$  vectors in the test data set gives the total predicted error

$$\begin{aligned} \ln L &= - \prod_{k=1}^{K=K} P(t_k|x_k, D) \\ &= \sum_{k=1}^{K=K} \left[ \frac{(T_k - \hat{t}_k)^2}{2\sigma_k^2} + \ln \sigma_k \right] \quad \dots \dots \dots \quad (6) \end{aligned}$$

where  $T_k$ ,  $\hat{t}_k$ , and  $\sigma_k$  are the target, prediction, and model predicted uncertainty, respectively, for the  $k$ th vector; an additive constant has been dropped. The measure  $\ln L$  is a dimensionless error, with more negative values indicating a better model. The values of  $\ln L$  for the Gaussian process models are listed in Table 2. While the 22D Gaussian process model gives a larger rms error than does the 12D Gaussian process model on the  $Ac_3$  problem, they have very similar  $\ln L$  values. In terms of the consistency of their predictions with their reported uncertainties, therefore, the two models are equally good.

The neural network gives slightly lower average errors than the Gaussian process for the 22D problems. However, it should be noted that many neural networks with different degrees of complexity and different initial weights were

tried before selecting the best, i.e. that which gave the smallest error on the test data set.<sup>1</sup> No such selection was done (or is necessary) with the Gaussian process, so the comparison is not entirely fair.

## **Conclusions**

The Gaussian process model has been introduced for empirically modelling the relationship between a set of input variables and an output variable. This model has been applied to the problem of predicting the temperature at which austenite starts to form  $Ac_1$  and the temperature at which austenite formation is completed  $Ac_3$ , during the continuous heating of a steel alloy. In contrast to previous work (GBMS), a reduced data set has been used by removing those trace elements believed to be largely irrelevant in determining  $Ac_1$  and  $Ac_3$  at the concentrations involved. Their irrelevance has been confirmed by analysis, as Gaussian process models trained on the original full data set (22 inputs) give very similar results to those of Gaussian process models trained on the reduced data set (12 inputs).

The Gaussian process model has the advantage over the neural network model that a decision regarding the number of hidden nodes and layers in the network is avoided. The neural network architecture must often be optimised by training a range of networks and comparing their performances on a separate validation data set. No such validation data set is required when training the Gaussian process, allowing all of the data to be used for training. Another advantage of the Gaussian process model is that its hyperparameters are more interpretable than the weights in a neural network. The present results have demonstrated that the Gaussian process model performs at least as well as the neural network model of GBMS,<sup>1</sup> and in many cases produced better predictions (for example with nickel) and smaller error bars (for example with silicon).

## Appendix

The predictive probability distribution from the Gaussian process model (equation (2)) is a univariate Gaussian with

mean  $\hat{t}$  and standard deviation  $\sigma_{\hat{t}}$  (equation (3)). These are given by (for example, Ref. 9).

where

$$k = [C(x_1, x_{N+1}), C(x_2, x_{N+1}), \dots, C(x_N, x_{N+1})] \quad . \quad (9)$$

and  $C$  is the covariance function (equation (4));  $C_N$  is the  $N \times N$  covariance matrix formed from the  $N$  training data points, the elements of which are  $C_{ij} = C$ ;  $x_1, x_2, \dots, x_N$  are the  $N$  input vectors in the training data set corresponding to the  $N$  outputs  $t_1, t_2, \dots, t_N$ ; and  $x_{N+1}$  is the input at which a prediction of  $t$  is required.

### **Acknowledgement**

The authors would like to thank Mark Gibbs for use of his Gaussian process software.

## References

1. L. GAVARD, H. K. D. H. BHADESHIA, D. J. C. MacKAY, and S. SUZUKI: *Mater. Sci. Technol.*, 1996, **12**, 453–463.
  2. C. K. I. WILLIAMS and C. E. RASMUSSEN: in ‘Neural information processing systems 8’, (ed. D. S. Touretzky *et al.*); 1996, Boston, MA, MIT.
  3. M. N. GIBBS: ‘Bayesian Gaussian processes for regression and classification’, PhD thesis, University of Cambridge, UK, 1998.
  4. R. M. NEAL: ‘Bayesian learning for neural networks’, No. 118 in ‘Lecture notes in statistics’; 1996, New York, NY, Springer.
  5. C. A. L. BAILER-JONES, T. J. SABIN, D. J. C. MacKAY, and P. J. WITHERS: in ‘Proceedings of the Australasia Pacific forum on intelligent processing and manufacturing of materials’, (ed. T. Chandra *et al.*), Vol. 2, 913–919; 1997, Brisbane, Watson Ferguson.
  6. C. A. L. BAILER-JONES, D. J. C. MacKAY, T. J. SABIN, and P. J. WITHERS: *Aust. J. Intell. Inf. Process. Syst.*, 1998, **5**, (1), 10–17.
  7. D. J. C. MacKAY: *Neural Comput.*, 1992, **4**, 415–447.
  8. A. O’HAGAN: *J. R. Stat. Soc.*, 1978, **B40**, 1–42.
  9. R. von MISES: ‘Mathematical theory of probability and statistics’; 1964, New York, NY, Academic Press.